

Article

Rejuvenation of Zr-Based Bulk Metallic Glasses by Ultrasonic Vibration-Assisted Elastic Deformation

Yan Lou *, Shenpeng Xv, Zhiyuan Liu and Jiang Ma

Guangdong Provincial Key Laboratory of Micro/Nano Optomechatronics Engineering, College of Mechatronics and Control Engineering, Shenzhen University, Shenzhen 518060, China;

Abstract: The rejuvenation of $Zr_{52.5}Cu_{17.9}Ni_{14.6}Al_{10}Ti_5$ bulk metallic glasses (BMGs) by ultrasonic vibration-assisted elastic deformation (UVEF) was studied herein. The UVEF-treated samples demonstrate an obvious rejuvenation and have a higher relaxation enthalpy and a smaller range of supercooled liquid regions than the as-cast samples. The fracture of the rejuvenated amorphous alloy is mainly ductile fracture, and shear deformation occurs in the deformation region. It is also found that as the amplitude increases, the free volume of the rejuvenated amorphous alloy increases, the yield strength and the elastic modulus decrease, and the formability increases. The free-volume content is used to characterize the degree of rejuvenation, and a mathematical model of the relationship between the ultrasonic amplitude and free volume is established. In addition, it is found that the ultrasonic vibration stress induces the additional free volume in the Zr-based bulk metallic glasses and improves the plasticizing behavior. The temperature rise caused by the ultrasonic thermal effect does not induce additional free volume.

Keywords: bulk metallic glasses (BMGs); rejuvenation; ultrasonic vibration-assisted elastic deformation (UVEF); free volume; plasticity

1. Introduction

Bulk metallic glasses (BMGs) are materials with excellent performance and mechanical properties, such as high yield strength [1], high toughness [2], high hardness [3] and exceptional “damage tolerance” [4,5]. However, the nonuniform deformation caused by the highly localized deformation at room temperature directly causes its brittleness [6,7], which has become the bottleneck for the widespread application of BMGs. Reducing the brittleness of BMGs has become a scientific issue that scholars have begun to pay attention to.

The rejuvenation of amorphous alloys occurs when BMGs are injected with high energy because it endows them with additional free volume and greater plasticity [8,9]. Therefore, rejuvenation of BMGs to reduce their brittleness and improve their plasticity at room temperature has attracted a lot of attention [10–12]. For example, J. Michler [13] conducted compression experiments on ion-radiated BMGs and found that they can increase the free-volume content of BMGs and enhance their plasticity. J. Das [14] utilized cold-rolled Zr-based BMGs at room temperature to overcome their inherent brittleness and make BMGs plastic from 0.5% to 15%. F. X. Li [15] discovered that during the elastic compression of $Zr_{35}Ti_{30}Be_{27.5}Cu_{7.5}$ BMGs at room temperature, the BMGs transitioned from mechanical relaxation to rejuvenation, thereby improving their plasticity. W. Guo [16] studied the rejuvenation of Zr–Cu–Al–Ni–Ta BMGs under cryogenic cycle treatment (DCT) and found that by adding more Ta, the BMGs can be restored to an elevated energy, and the compressive fracture strength and plastic strain increased with increasing Ta content. Through plastic deformation under triaxial compression at room temperature,

Y. Li and A.L. Greer [4] rejuvenated BMGs samples and found that the rejuvenated amorphous material showed excellent plastic deformation ability. However, elastic loading [17], ion radiation [18], thermal cycling [19,20], and plastic deformation [21] methods require a substantial amount of time to rejuvenate the BMGs, and during this time, a relaxation effect inevitably occurs, weakening the rejuvenation effect.

In addition, ultrasonic vibration-assisted has an ultrasonic stress effect and ultrasonic thermal effect. P. Chen [22] used ultrasonic vibration to process a Ti-based amorphous powder to make nanocrystalline bulk materials. The amorphous powder was crystallized by the frictional heat generated during the ultrasonic vibration and then welded to form a bulk nanocrystalline material. J. Ma et al. [23] used supersonic vibration to stamp BMGs and found that this forming method completed thermoplastic forming in seconds and largely avoided the time-dependent crystallization and oxidation processes, thus avoiding the risk of crystallization that occurs during traditional heat processing. N. Li et al. [24] conducted uniaxial tensile and compression experiments on Zr-based amorphous alloys under the action of a vibration field and found that with increasing vibration frequency, the free-volume content of the amorphous alloy increased and the flow unit volume decreased, which caused the flow viscosity to decrease and the micro-forming ability to increase. However, there are no reports that specifically analyze the influence of ultrasonic vibration stresses and ultrasonic thermal effects on amorphous properties.

A novel method of ultrasonic vibration-assisted elastic deformation (UVEF) was developed that can successfully and rapidly rejuvenate Zr-based BMGs within 8 s. It was found that ultrasound-assisted vibration can rapidly increase the internal energy of BMGs and quickly drive the loosely packed atoms in BMGs to high-energy regions, thereby driving additional areas with free volume and rheological units to form shear bands. These processes result in the rapid rejuvenation of BMGs and prevent the time-dependent crystallization and relaxation phenomena. In addition, the thermodynamics, mechanical properties and fracture morphology of the rejuvenated UVEF-treated samples were analyzed. It was found that as the amplitude increased, the yield strength and elastic modulus of the UVEF-treated samples decreased, and the plasticity was greatly improved. The free volume was used to characterize the degree of rejuvenation of the amorphous alloys herein, and a mathematical model of the relationship between the ultrasonic amplitude and the free volume of the rejuvenated BMGs was established. The effects of the temperature rise and stress caused by the ultrasonic vibration on the rejuvenation properties of BMGs were analyzed. These findings provide a convenient and fast method to reduce the room-temperature brittleness of BMGs and improve their plasticity.

2. Experimental Methods

2.1. Sample Preparation

The experimental material is an amorphous alloy with an alloy composition of $\text{Zr}_{52.5}\text{Cu}_{17.9}\text{Ni}_{14.6}\text{Al}_{10}\text{Ti}_5$ (atomic percentage). The raw materials of metals Zr, Cu, Ni, Al, and Ti with a purity of 99.9% or more are prepared according to the nominal composition. An electric arc furnace is used to melt the master alloy, and then a copper die suction casting method is used to prepare rod-shaped amorphous particles with a diameter of $\Phi 2$ mm. A low-speed diamond cutting machine is used to process a cylindrical sample with dimensions of $\Phi 2$ mm \times 4 mm. The ends of the cylinder are also polished to ensure that both ends are parallel to each other and orthogonal to the centerline of the cylinder. The sample was analyzed with X-ray diffraction (XRD, Bruker D8 Advance, Bruker, Karlsruhe, Germany) to ensure that the sample is in an amorphous state.

2.2. UVEF Processing

The experiments herein use a homemade ultrasonic vibration-assisted compression test platform. The ultrasonic vibration-assisted device is installed on a Zwick Z050 tensile testing machine (Zwick Roell Group, Ulm, Germany). The maximum power of the ultrasonic system is 1500 W, and the vibration frequency is 20 kHz. Due to the limitation of the experimental conditions, the ultrasonic frequency in

UVEF can be calculated:

where t_{pl} is the time of preloading, t_{ul} is the ultrasonic loading time, S is the distance between the initial punch and the upper surface of the sample, and V is the preloading speed. S_{pl} and V_{pl} were taken as 0.5 mm and 0.1 mm/s, respectively. A strain rate of " $\dot{\epsilon}$ = 0.01 s⁻¹" and a strain of " ϵ = 2%" were taken as 0.5 mm and 0.1 mm/s, respectively. A strain rate of 0.01 s⁻¹ and a strain of 2% applied were applied to ensure that compression that compression is within the within amorphous/amorphous elastic deformation/elastic deformation range, and range, BMGs and can be BMGs rejuvenate can be rejuvenated within 8 s. Five within BMGs samples Five BMGs were samples repeatedly were compressed repeatedly under compressed each deformation under each process deformation condition process' condition.

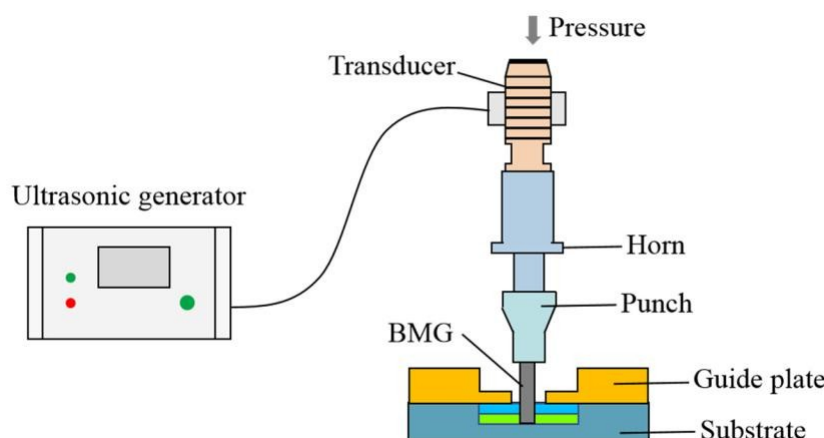


Figure 1.. Ultrasonic vibration--assisted elastic deformation diagram.

2.3. Hot-Compressed Elastic Deformation (HEF) Experiment

2.3. Hot-Compressed Elastic Deformation (HEF) Experiment

To specialized analyze the effects of the temperature rise and stress produced during the ultrasonic To specialized analyze the effects of the temperature rise and stress produced during the vibration on the rejuvenation properties of the amorphous alloys, we eliminate the effect of ultrasonic vibration on the rejuvenation properties of the amorphous alloys, we eliminate the effect stress, and only the effect of temperature rise is studied separately. The temperature rise at different of ultrasonic stress, and only the effect of temperature rise is studied separately. The temperature rise amplitudes is obtained according to previous research results [25]. That is, amplitudes of 19, 27, 36, at different amplitudes is obtained according to previous research results [25]. That is, amplitudes of and 43 μm correspond to temperature increases of 80, 150, 200, and 270 $^{\circ}\text{C}$. HEF experiments at the 19, 27, 36, and 43 μm correspond to temperature increases of 80, 150, 200, and 270 $^{\circ}\text{C}$. HEF corresponding temperatures are performed on the thermal simulation machine (Gleeble3800, DSI, experiments at the corresponding temperatures are performed on the thermal simulation machine Austin, TX, USA). The corresponding strain rate and strain are consistent with the UVEF experiment (Gleeble3800, DSI, Austin, TX, USA). The corresponding strain rate and strain are consistent with the and are 0.01 s^{-1} and 2%, respectively. Five BMGs samples are repeatedly hot-compressed under each UVEF experiment and are 0.01 s^{-1} and 2%, respectively. Five BMGs samples are repeatedly hot-deformation condition.

compressed under each deformation condition.

2.4. Analytical Testing

2.4. Analytical Testing

To study the properties of the Zr-based BMGs samples, a series of analytical tests are performed on To study the properties of the Zr-based BMGs samples, a series of analytical tests are performed them. XRD (Bruker D8 Advance, Bruker, Karlsruhe, Germany) is used to determine the crystallization on them. XRD (Bruker D8 Advance, Bruker, Karlsruhe, Germany) is used to determine the of the samples. The scanning range is 20 ~ 80°, the step size is 0.02° step 1, and the scanning speed is crystallization of the samples. The scanning range is 20° ~ 80°, the step size is 0.02° step-1, and the 12 min 1. The Vickers microhardness test (BUEHLER 5103, Buehler, Lake Blu, IL, USA; ASTM 92-82, scanning speed is 12° min-1. The Vickers microhardness test (BUEHLER 5103, Buehler, Lake Bluff, IL

USA; ASTM E92-82, West Conshohocken, PA, USA) is used to determine the hardness of the samples, the diamond indenter was pressed into the surface of the specimen along its axial direction with a

PerkinElmer DSC8000, thermodynamic PerkinElmer

tempera

3. Results and Discussion

Figure 2 is a comparison of the XRD patterns of the as-cast and UVEF-treated samples. It can be found that the XRD diffraction peaks of the UVEF-treated samples are consistent with those of the as-cast and UVEF-treated samples. It can be found that the XRD diffraction peaks of the UVEF-treated samples are consistent with those of the as-cast samples. There are broad diffusion peaks without any obvious crystalline peaks in both as-cast samples. There are broad diffusion peaks without any obvious crystalline peaks in both cases, which indicates that the as-cast and UVEF-treated samples are all amorphous, and ultrasonic vibration-assisted elastic deformation does not cause the amorphous material to crystallize. Regarding the vibration-assisted elastic deformation does not cause the amorphous material to crystallize. naming convention, the UVEF-19 sample is an amorphous sample treated by ultrasonic vibration-assisted elastic deformation with an amplitude of 19 m.

ultrasonic vibration-assisted elastic deformation with an amplitude of 19 μm .



assisted- assistedelasticeformationlasticdeformation(UVEF)-treated(UVEF)samples-treated. samples.

To further confirm the amorphous properties of the as-cast and UVEF-treated samples, high-resolution TEM is used to obtain images of the microstructure of the sample, of which sample is shown in Figure 3. No nanocrystals are found in the as-cast samples, and the microstructure of all samples shows a labyrinth-like characteristic similar to that of an amorphous state, which is consistent with the XRD test results.

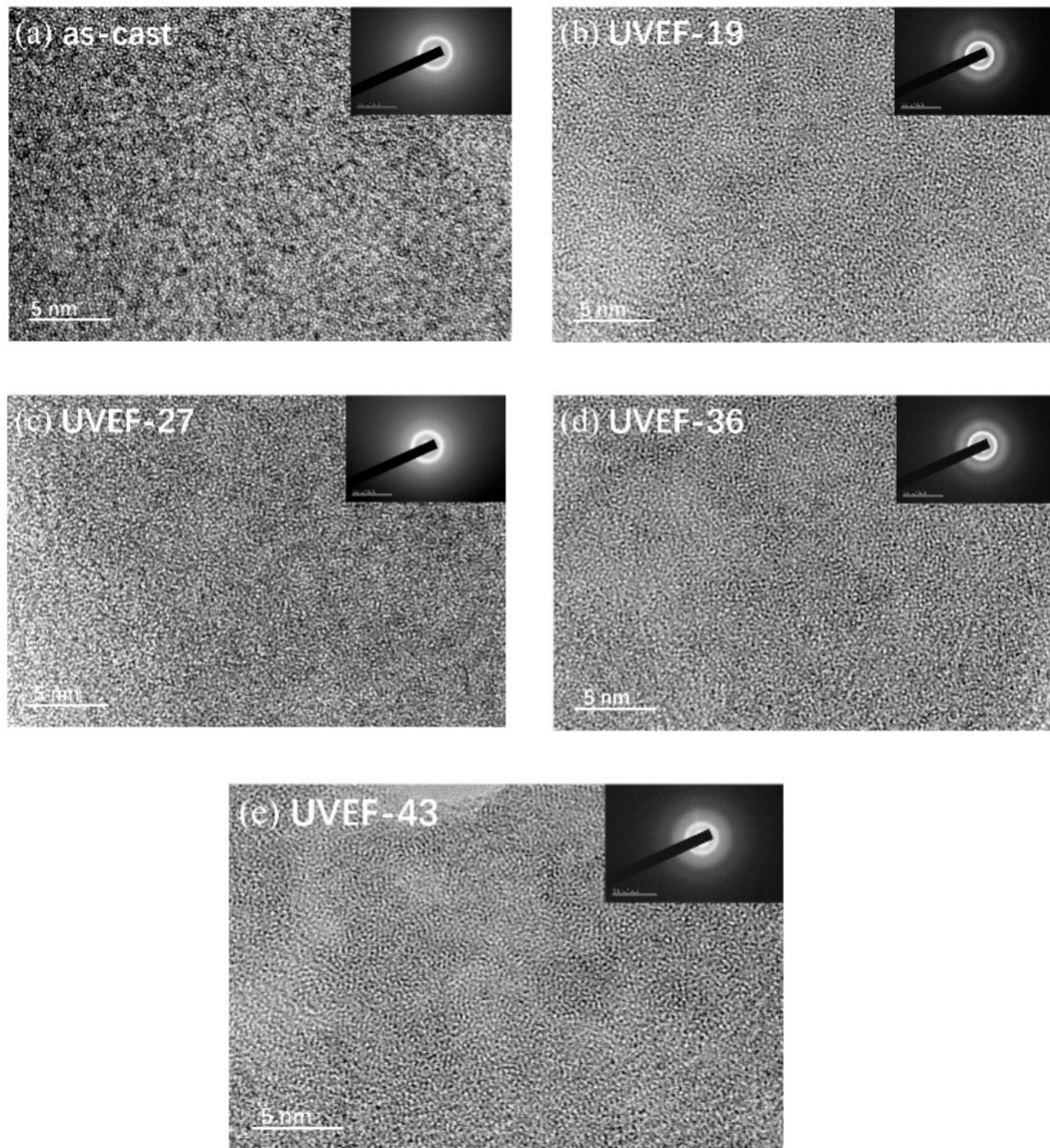


Figure 3. Transmission electron microscopy (TEM) images of the as-cast sample and the UVEF-treated samples: (a) as-cast; (b) UVEF-19; (c) UVEF-27; (d) UVEF-36; and (e) UVEF-43.

3.1. Thermodynamics Analysis

3.1.1. Thermodynamics Analysis

The as-cast and UVEF-treated samples are analyzed by DSC, and the thermodynamic properties of the samples are obtained from the DSC curve. As shown in Figure 4, the DSC curves of all samples show an endothermic phenomenon starting from the T_g temperature, which is a characteristic of glass transition, and then exhibit an exothermic phenomenon corresponding to the crystallization behavior to the T_x temperature. The values of T_g and T_x for as-cast and UVEF treated samples as shown in Table 1.

1.

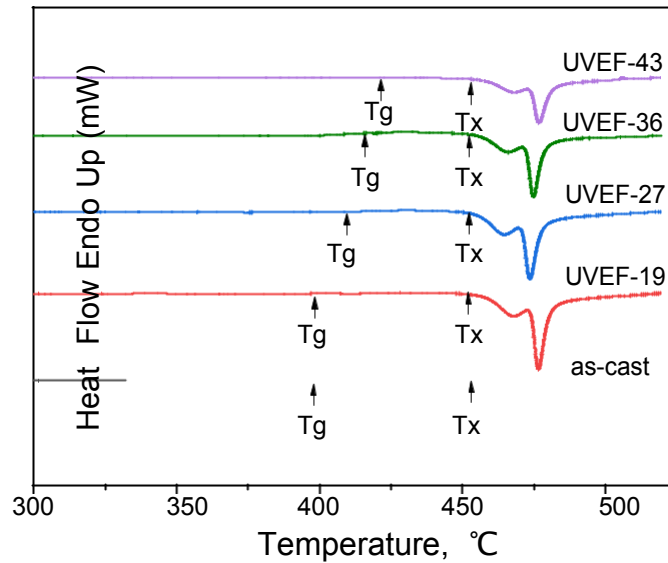


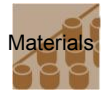
Figure 4. Differential scanning calorimetry (DSC) curves of the as-cast and UVEF-treated samples.

Table 1. The values of the glass transition temperature T_g and the crystallization temperature T_x for as-cast and UVEF-treated samples.

Sample	T_g (K)	T_g (K)	T_x (K)	T_x (K)	ΔT (K)
As-cast	397	397	452	452	55
UVEF-19	398	398	452	452	54
UVEF-27	410	410	453	453	43
UVEF-36	416	416	453	453	37
UVEF-43	422	422	454	454	32

Compared with that of the as-cast sample, the crystallization temperature T_x of the UVEF-treated sample shows only slight fluctuations, roughly in the range of $453 \pm 1^\circ\text{C}$, while the glass transition temperature T_g showed an upward trend with increasing ultrasonic amplitude. This shows that an increased amplitude ultrasonic vibration can increase the glass transition temperature T_g of the amorphous alloy and reduce the range of its supercooled liquid region. According to the Spaepen plastic deformation mechanism, BMGs will undergo uneven plastic deformation at high strain rates, resulting in a large number of shear bands. The arrangement density of atoms near the shear zone is less than that of the matrix, so a large amount of free volume is concentrated in the shear zone at this time, causing the increase of atomic mobility, the deterioration of the thermal stability of the material, and the increase of T_g [8,26].

Because of the structural relaxation, the amorphous alloy exhibits exothermic phenomena during continuous heating to the T_g (Figure 5). The larger the value of free volume change (ΔV_f) is, the greater the relaxation enthalpy ΔH of the as-cast and UVEF-treated samples during DSC thermodynamic analysis. The ΔH is calculated by calculating the integrated area of the exothermic peak, and the change in ΔH reflects the disorder of the atomic arrangement [28]. It is found that with an increase in the ultrasonic amplitude, the ΔH value of the UVEF-treated sample increases significantly. The larger the ΔH value is, the greater the free volume V_f value of the amorphous alloy. This is because under the vibration load, the UVEF-treated samples were injected with a high energy and the atom diffusion increases. The atomic arrangement also becomes looser, and the larger the amplitude is, the stronger the atom diffusion and the higher the amorphous energy. This result also shows that the degree of rejuvenation of the UVEF-treated sample increases.



materials



8 samples obtained by SEM. All samples fracture along the maximum shear stress plane at an angle of approximately 45° to the loading axis. The microstructure was not uniform across the fracture surface, and the fractures of as-cast samples are obviously in the shape of veins, mountains, and rivers (Figure 8a), which is a typical brittle fracture morphology. The fracture surface morphology of the UVEF-treated samples is mainly ductile fracture (Figure 8b-e). The fracture surface has a large number of vein-like textures. This texture is due to the shear zone breaking during the stress loading process. The local melting phenomenon caused by the instantaneous release indicates that the material has undergone shear deformation in the region, which is consistent with the experimental results in Figure 6a, indicating that the ultrasonic vibration-assisted elastic deformation process rejuvenates the amorphous alloys.

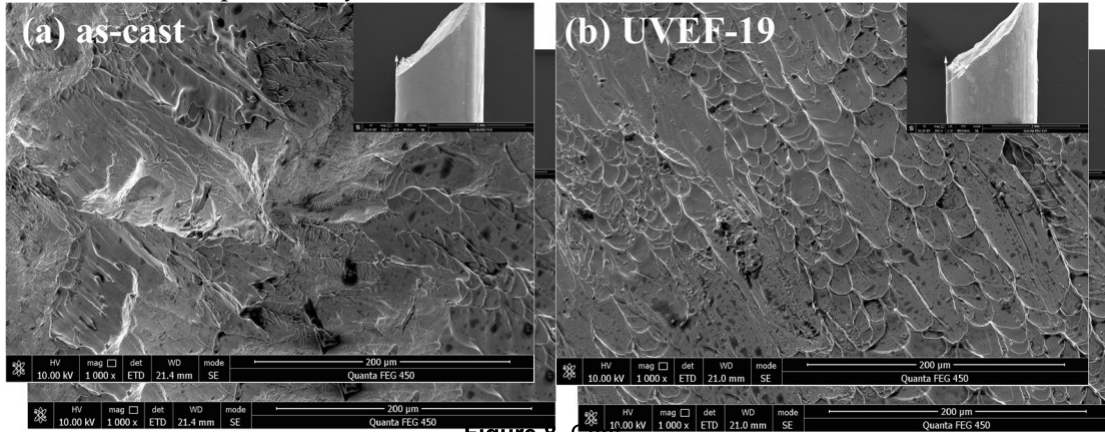


Figure 8. Cont.

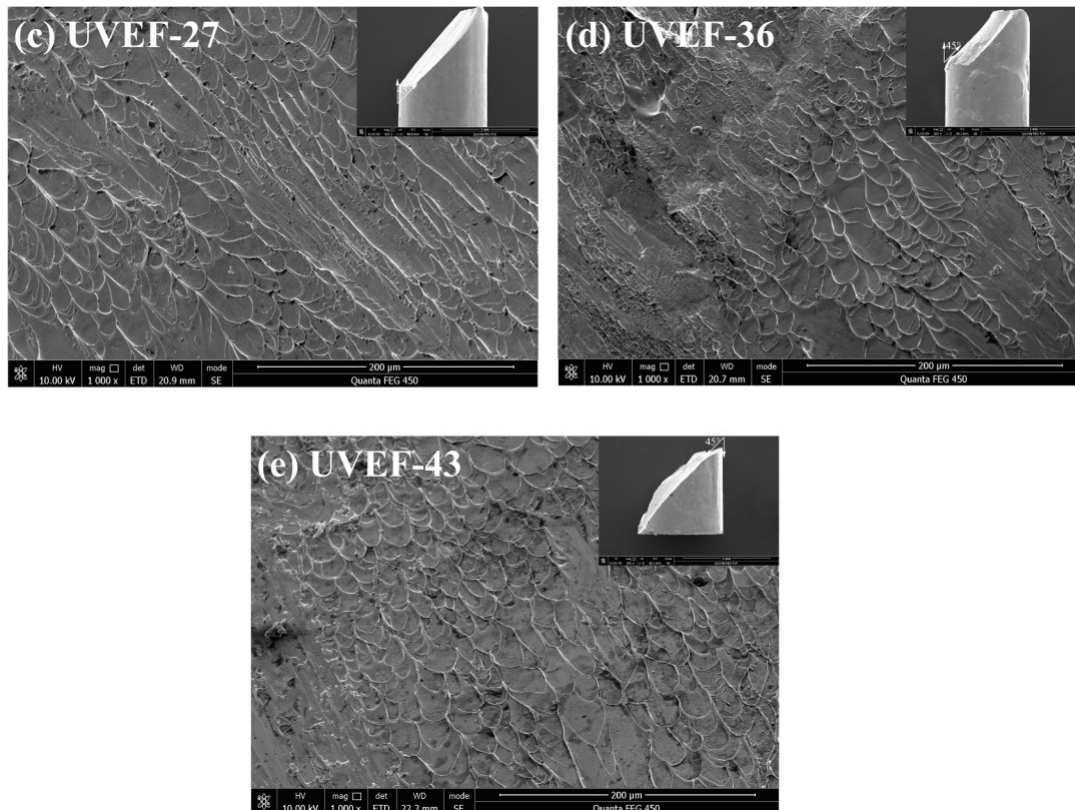


Figure 8. Compressive fracture micromorphology of the as-cast and UVEF-treated samples: (a) as-cast; UVEF-36; and (e) UVEF-43.

3.5. Properties of the Hot-Compressed Elastic Deformation Treated Sample

3.5. Properties of the Hot-Compressed Elastic Deformation Treated Sample

From a comparison of XRD patterns of hot-compressed elastic deformation (HEF)-treated samples in Figure 9a, it can be found that the patterns of HEF-treated samples show broad elastic deformation peaks and (HEF)-no obvious treated samples crystalline peaks. Figure 9a, it can be found that the HEF-treated samples still have an amorphous broad diffraction. Regarding peaks and the no sample obvious naming crystalline convention, peaks, HEF which 80 refers to prove to amorphous that the HEF samples treated processed samples by a hot still compressed all amorphous elastic. Regarding deformation that sample temperature naming of convention, 80°C. The HEF microscopic 80 refers to morphology to amorphous observed samples with processed TEM shown by hot-compressed Figure 9b indicates elastic deformation that the HEF at treated temperature sample shows of 80°C. a maze-like amorphous morphology structure, observed and no with nanocrystals TEM shown are found in Figure. 9b indicates that the HEF-treated sample shows a maze-like amorphous structure, Figure and 10 shows nanocrystal microhardness are found values. of the as-cast and HEF-treated samples. The microhardness

value does not decrease with increasing temperature. Compared with the UVEF-treated samples (Figure 7), the effect of deformation on the amorphous particles is the opposite. Indicating that only an elastic deformation treatment with increasing temperature does not induce an increase in the amount of free volume. It is also found that the relaxation enthalpy ΔH of the HEF-treated sample is slightly larger than that of the as-cast sample (Figure 10b), but as the temperature increases, the relaxation enthalpy ΔH of the HEF-treated sample essentially does not change, indicating that its free volume does not change with increasing temperature. It also further shows that the aspect of the ultrasonic vibration-assisted elastic deformation process that creates additional free volume is the ultrasonic vibration stress, not the temperature rise caused by the ultrasonic thermal effect. The ultrasonic vibration stress can create additional free volume and improve the rejuvenation degree of amorphous alloys [31].

Figure 9. (a) Comparison of XRD patterns of as-cast and hot-compressed elastic deformation (HEF) - treated samples, and (b) TEM image of HEF-270 treated sample.

Figure 10a shows the microhardness values of the as-cast and HEF-treated samples. The microhardness value does not decrease with increasing temperature. Compared with the UVEF-treated samples (Figure 7), the effect of deformation on the amorphous particles is the opposite,

samples in Figure 9a, it can be found that the HEF-treated samples have broad diffusion peaks and no obvious crystalline peaks, which proves that the HEF-treated samples are still all amorphous. Regarding the sample naming convention, HEF-80 refers to amorphous samples processed by hot-compressed elastic deformation at a temperature of 80 °C. The microscopic morphology observed Materials with TEM 2020 shown, 13, 4397 in Figure 9b indicates that the HEF-treated sample shows a maze-like amorphous structure, and no nanocrystals are found.

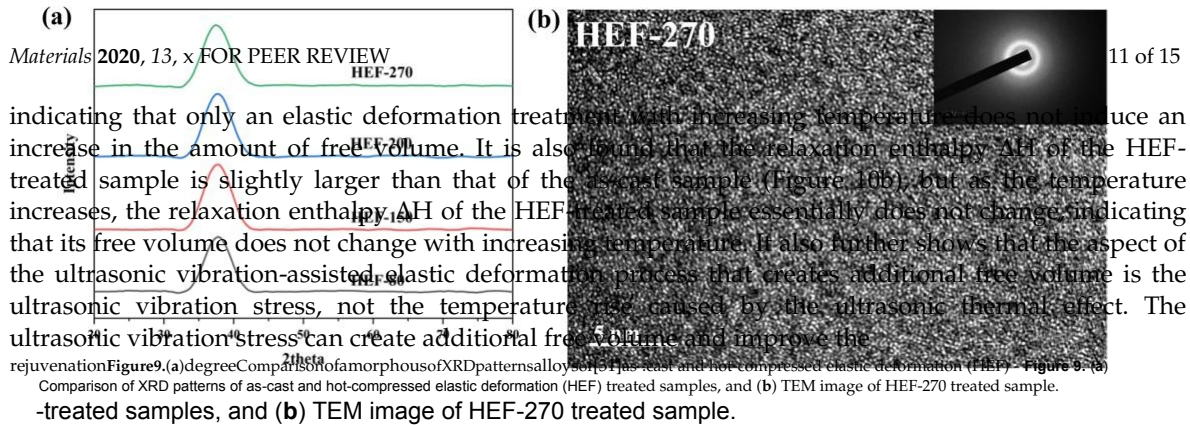


Figure 10a shows the microhardness values of the as-cast and HEF-treated samples. The microhardness value does not decrease with increasing temperature. Compared with the UVEF-treated samples (Figure 7), the effect of deformation on the amorphous particles is the opposite,

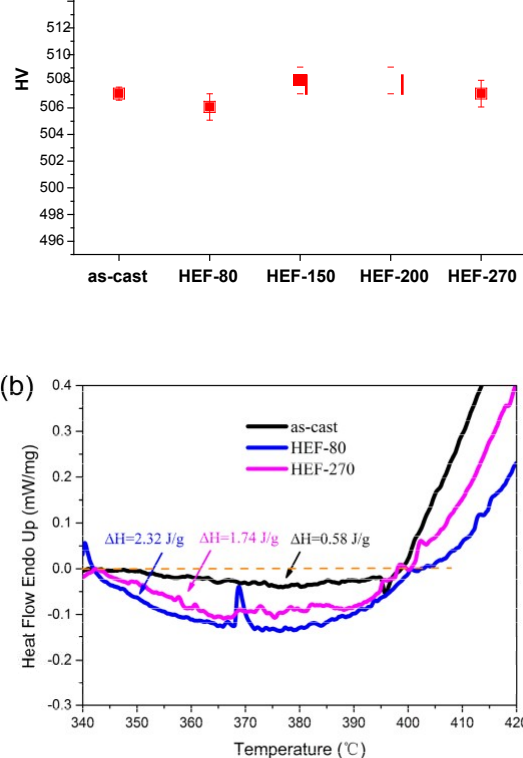


Figure 10. (a) Comparison of microhardness of the as-cast and HEF-treated samples and (b) comparison of relaxation enthalpies of the as-cast and HEF-treated samples.

It is found that the fracture stress-strain curve of the HEF-treated samples has a very short yield stage before fracture, approximately 0.3% of the strain, and then the samples immediately fracture. It is found that the fracture strength, elastic modulus, and plastic strain of (Figure 11). At the same time, it is found that the yield strength of the HEF-treated sample essentially did not change with increasing temperature. This also verifies the results of Figure 10. The increase in the plasticity of the UVEF-treated sample is caused by an increase in the free volume induced by the ultrasonic vibration stress, which promotes the rejuvenation of the amorphous alloy. The ultrasonic thermal effect that causes a temperature increase does not increase the plasticity of the amorphous sample. This is because the maximum temperature rise caused by the ultrasonic thermal effect in this study is 270 °C, which is far lower than the T_g of the Zr-based BMGs.

BMGs. Therefore, at low temperatures, an increase in the temperature cannot increase the free volume. The ultrasonic vibration is the main reason for the increase in the free volume and the degree of rejuvenation demonstrated herein [31].

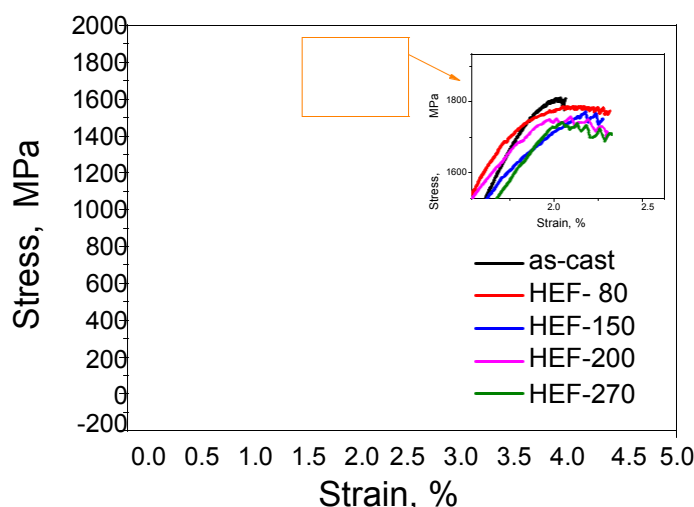


Figure 11. Fracture stress-strain curve of the as-cast and HEF-treated samples.

3.6. Mathematical Model of the Relationship between Ultrasonic Amplitude And Free Volume

3.6. Mathematical Model of the Relationship between Ultrasonic Amplitude And Free Volume

The shear phase transformation zone (STZ) model [32] is widely used to describe the physical process of plastic deformation of amorphous alloy materials. This STZ model is applicable whether the deformation is transient or time-dependent and uniform or nonuniform. Generally, shear deformation is preferentially activated in areas with an increased free volume. Therefore, an increased free volume leads to easier and more shear deformation, which in turn leads to better plasticity. It is deduced from this that the BMGs with an increased free volume show a decreased resistance to any form of deformation. The ultrasonic amplitude leads to a high-energy state, which increases the free volume and increases the degree of rejuvenation of amorphous alloys.

It is deduced from this that the BMGs with an increased free volume show a decreased resistance to any form of deformation. The ultrasonic amplitude leads to a high-energy state, which increases the free volume and increases the degree of rejuvenation of amorphous alloys.

the free volume and increases the degree of rejuvenation of amorphous alloys. To quantify the effect of the ultrasonic amplitude on the rejuvenation degree of the amorphous alloys, the amount of free volume in the UVEF-treated samples is theoretically calculated based on the free volume formula [33]:

alloys, so the amount of free volume in the UVEF-treated samples is theoretically calculated based

$$v_f = v_f^* \exp\left(-\frac{2s}{v_f^*} \dot{\gamma}\right) \quad (2)$$

strain. Also:

$$v_f^* = \frac{1}{C} \exp\left(-\frac{k_t \ln \dot{\gamma} + l}{D}\right) \quad (3)$$

where C is the fitting parameter, v_f^*

is the steady-state free volume, $\dot{\gamma}$ is the shear strain rate, and s

is the strain. Also:

$$v_{fe} = \frac{T - T_0}{DT_0} \quad (4)$$

where v_{fe} is the equilibrium free volume; k = 26.6 + 0.044T and l = 43.9 + 0.082T represent

temperature-related parameters [33]; D is the brittleness index of the BMGs, which is taken as 18.5; and T_0 is the Vogel-Fulcher temperature, $T_0 = 2/3T_g$.

The amount of free volume of the UVEF-treated sample can be obtained according to Equation (2), as shown in Figure 12. It can be found that the larger the amplitude of the UVEF-treated sample is, the

$$v_f = \frac{T - T_0}{DT_0} \exp\left(-\frac{2s}{v_f^*} \dot{\gamma}\right) \quad (4)$$

where v_{fe} is the equilibrium free volume; $k_t = 26.6 + 0.044T$ and $l = 43.9 + 0.082T$ represent temperature-related parameters [33]; D is the brittleness index of the BMGs, which is taken as 18.5; and T_0 is the Vogel-Fulcher temperature, $T_0 = 2/3T_g$.

fitting is 0.99983, the mathematical model to obtain the ultrasonic amplitude (A) and free volume (v_f) is obtained as follows:

$$v_f = 7.9857 - 0.20477A + 0.01216A^2 \quad (5)$$

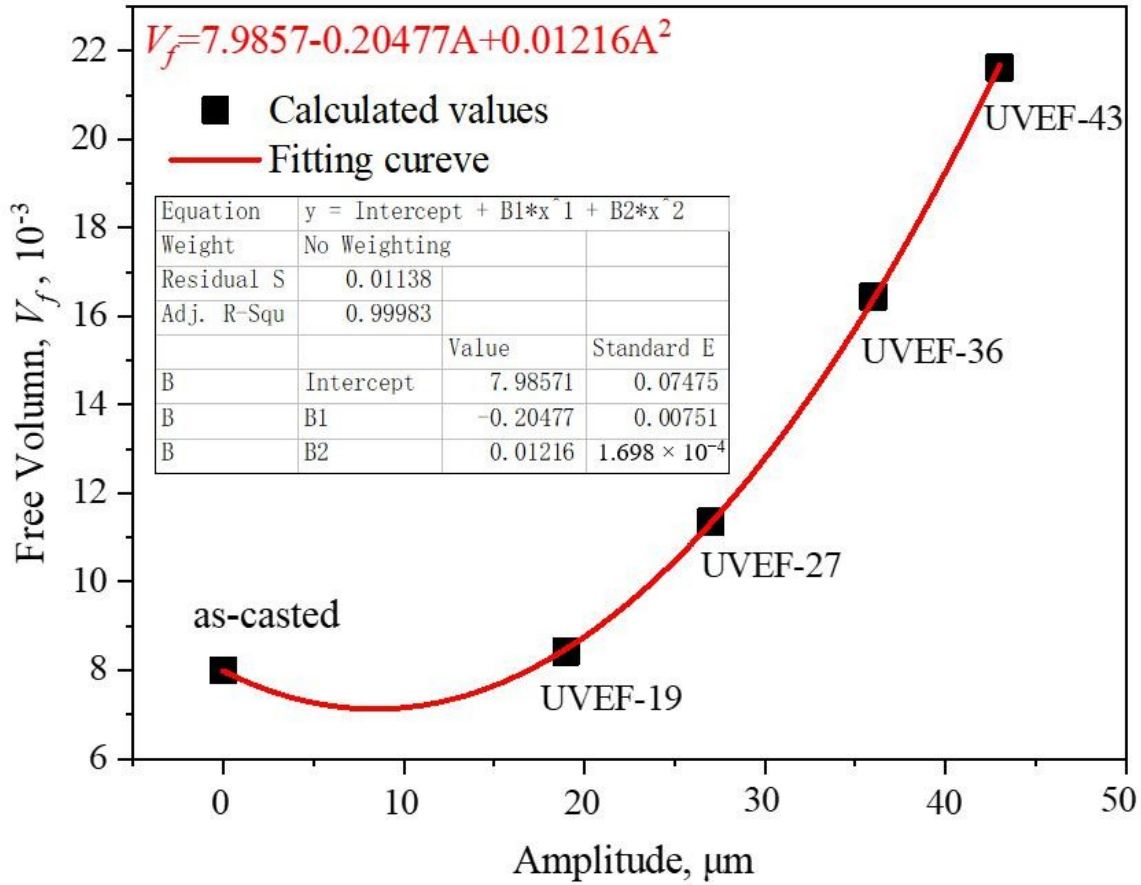


Figure 12. Theoretical model of the relationship between the free volume and amplitude of UVEF-treated samples.

As the amplitude increases, the amount of free volume increases sharply, indicating that the greater the ultrasonic energy is, the greater the degree of amorphous rejuvenation.

4. Conclusions

Compared with metallic glass rejuvenation methods such as elastic loading and ion radiation, UVEF has a short processing time (8s), will not cause damage, and is also controllable. It is found that the relaxation enthalpy increases and the range of the supercooled liquid region decreases when Zr based metallic glasses are UVEF-treated at room temperature. With the increase of amplitude, the free volume and the formability of the UVEF-treated sample increase, and the yield strength and elastic modulus decrease. Ultrasonic vibration stress is the main reason for the increase in the free volume of Zr-based BMGs.

Author Contributions: Conceptualization, Y.L.; methodology, Y.L. and Z.L.; validation, Z.L.; formal analysis, Y.L.; investigation, S.X.; resources, Y.L.; data curation, Y.L.; writing—original draft preparation, S.X.; writing—review and editing, Y.L.; visualization, Z.L.; supervision, J.M.; project administration, Y.L.; funding acquisition, Y.L. and Z.L. All authors have read and agreed to the published version of the manuscript.

Funding: This research was funded by National Natural Science Foundation of China, grant number 51675347 and 5197114; and Science and Technology Innovation Commission of Shenzhen, grant number JCYJ20190808152409578.

Conflicts of Interest: The authors declare no conflict of interest

References

1. Inoue, A. Stabilization of metallic supercooled liquid and bulk amorphous alloys. *Acta Mater.* **2000**, *48*, 279–306. [[CrossRef](#)]
2. Telford, M. The case for bulk metallic glass. *Mater. Today* **2004**, *7*, 36–43. [[CrossRef](#)]
3. Demetriou, M.D.; Launey, M.E.; Garrett, G.; Schramm, J.P.; Hofmann, U.C.; Johnson, W.L.; Ritchie, R.O. A damage-tolerant glass. *Nat. Mater.* **2011**, *10*, 123–128. [[CrossRef](#)] [[PubMed](#)]
4. Pan, J.; Ivanov, Y.P.; Zhou, W.H.; Li, Y.; Greer, A.L. Strain-hardening and suppression of shear-banding in rejuvenated bulk metallic glass. *Nature* **2020**, *578*, 559–562. [[CrossRef](#)] [[PubMed](#)]
5. Deng, X.; Chen, S.; Hu, Q.; Xie, S.; Zou, J.; Sial, M.A.Z.G.; Zeng, X. Excellent room-temperature mechanical properties in the high glass-forming Zr Cu Ni Al Nb alloy system. *Mater. Res. Express* **2019**, *6*, 086551. [[CrossRef](#)]
6. Schroers, J. Processing of Bulk Metallic Glass. *Adv. Mater.* **2009**, *22*, 1566–1597. [[CrossRef](#)]
7. Zhang, T.; Meng, X.; Wang, C.; Li, L.; Yang, J.; Li, W.; Li, R.; Zhang, Y. Investigations of new bulk metallic glass alloys fabricated using a high-pressure die-casting method based on industrial grade Zr raw material. *J. Alloys Compd.* **2019**, *792*, 851–859. [[CrossRef](#)]
8. Spaepen, F. A microscopic mechanism for steady state inhomogeneous flow in metallic glasses. *Acta Met.* **1977**, *25*, 407–415. [[CrossRef](#)]
9. Nieh, T.; Schuh, C.; Wadsworth, J.; Li, Y. Strain rate-dependent deformation in bulk metallic glasses. *Intermetallics* **2002**, *10*, 1177–1182. [[CrossRef](#)]
10. Saida, J.; Yamada, R.; Wakeda, M.; Ogata, S. Thermal rejuvenation in metallic glasses. *Sci. Technol. Adv. Mater.* **2017**, *18*, 152–162. [[CrossRef](#)]
11. Tong, Y.; Iwashita, T.; Dmowski, W.; Bei, H.; Yokoyama, Y.; Egami, T. Structural rejuvenation in bulk metallic glasses. *Acta Mater.* **2015**, *86*, 240–246. [[CrossRef](#)]
12. Liang, S.-X.; Jia, Z.; Liu, Y.-J.; Zhang, W.; Wang, W.; Lu, J.; Zhang, L. Compelling Rejuvenated Catalytic Performance in Metallic Glasses. *Adv. Mater.* **2018**, *30*, 223–234. [[CrossRef](#)] [[PubMed](#)]
13. Raghavan, R.; Boopathy, K.; Ghisleni, R.; Pouchon, M.; Ramamurty, U.; Michler, J. Ion irradiation enhances the mechanical performance of metallic glasses. *Scr. Mater.* **2010**, *62*, 462–465. [[CrossRef](#)]
14. Lee, M.-H.; Lee, K.; Das, J.; Thomas, J.; Kühn, U.; Eckert, J. Improved plasticity of bulk metallic glasses upon cold rolling. *Scr. Mater.* **2010**, *62*, 678–681. [[CrossRef](#)]
15. Zhang, M.; Wang, Y.M.; Li, F.X.; Jiang, S.Q.; Li, M.Z.; Liu, L. Mechanical Relaxation-to-Rejuvenation Transition in a Zr-based Bulk Metallic Glass. *Sci. Rep.* **2017**, *7*, 625. [[CrossRef](#)]
16. Guo, W.; Shao, Y.; Saida, J.; Zhao, M.; Lü, S.; Wu, S. Rejuvenation and plasticization of Zr-based bulk metallic glass with various Ta content upon deep cryogenic cycling. *J. Alloys Compd.* **2019**, *795*, 314–318. [[CrossRef](#)]
17. Lee, S.-C.; Lee, C.-M.; Yang, J.-W.; Lee, J.-C. Microstructural evolution of an elastostatically compressed amorphous alloy and its influence on the mechanical properties. *Scr. Mater.* **2008**, *58*, 591–594. [[CrossRef](#)]
18. Brechtel, J.; Wang, H.; Kumar, N.; Yang, T.; Lin, Y.-R.; Bei, H.; Neuefeind, J.; Dmowski, W.; Zinkle, S. Investigation of the thermal and neutron irradiation response of BAM-11 bulk metallic glass. *J. Nucl. Mater.* **2019**, *526*, 151771. [[CrossRef](#)]
19. Ketov, S.V.; Sun, Y.H.; Nachum, S.; Lu, Z.; Checchi, A.; Beraldin, A.R.; Bai, H.Y.; Wang, W.H.; Louzguine-Luzgin, D.V.; Carpenter, M.A.; et al. Rejuvenation of metallic glasses by non-a ne thermal strain. *Nature* **2015**, *524*, 200–203. [[CrossRef](#)]
20. Guo, W.; Yamada, R.; Saida, J. Rejuvenation and plasticization of metallic glass by deep cryogenic cycling treatment. *Intermetallics* **2018**, *93*, 141–147. [[CrossRef](#)]
21. Dmowski, W.; Yokoyama, Y.; Chuang, A.; Ren, Y.; Umemoto, M.; Tsuchiya, K.; Inoue, A.; Egami, T. Structural rejuvenation in a bulk metallic glass induced by severe plastic deformation. *Acta Mater.* **2010**, *58*, 429–438. [[CrossRef](#)]
22. Chen, P.; Liao, W.-B.; Liu, L.H.; Luo, F.; Wu, X.Y.; Li, P.J.; Yang, C.; Yan, M.; Liu, Y.; Zhang, L.; et al. Ultrafast consolidation of bulk nanocrystalline titanium alloy through ultrasonic vibration. *Sci. Rep.* **2018**, *8*, 801. [[CrossRef](#)] [[PubMed](#)]